

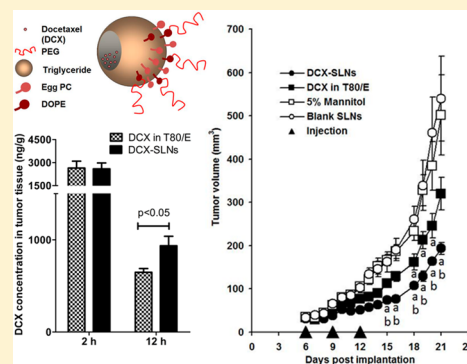
# Solid Lipid Nanoparticle Formulations of Docetaxel Prepared with High Melting Point Triglycerides: *In Vitro* and *In Vivo* Evaluation

Youssef Wahib Naguib,<sup>†</sup> B. Leticia Rodriguez,<sup>†</sup> Xinran Li,<sup>†</sup> Stephen D. Hursting,<sup>‡</sup> Robert O. Williams, III,<sup>†</sup> and Zhengrong Cui<sup>\*†</sup>

<sup>†</sup>Pharmaceutics Division, College of Pharmacy, and <sup>‡</sup>Department of Nutritional Sciences, College of Natural Sciences, The University of Texas at Austin, Austin, Texas 78712 United States

**ABSTRACT:** Docetaxel (DCX) is a second generation taxane. It is approved by the U.S. Food and Drug Administration for the treatment of various types of cancer, including breast, non-small cell lung, and head and neck cancers. However, side effects, including those related to Tween 80, an excipient in current DCX formulations, can be severe. In the present study, we developed a novel solid lipid nanoparticle (SLN) composition of DCX. Trimyristin was selected from a list of high melting point triglycerides as the core lipid component of the SLNs, based on the rate at which the DCX was released from the SLNs and the stability of the SLNs. The trimyristin-based, PEGylated DCX-incorporated SLNs (DCX-SLNs) showed significantly higher cytotoxicity against various human and murine cancer cells in culture, as compared to DCX solubilized in a Tween 80/ethanol solution. Moreover, in a mouse model with pre-established tumors, the new DCX-SLNs were significantly more effective than DCX solubilized in a Tween 80/ethanol solution in inhibiting tumor growth without toxicity, likely because the DCX-SLNs increased the concentration of DCX in tumor tissues, but decreased the levels of DCX in major organs such as liver, spleen, heart, lung, and kidney. DCX-incorporated SLNs prepared with one or more high-melting point triglycerides may represent an improved DCX formulation.

**KEYWORDS:** SLNs, *in vitro* release, cytotoxicity, caspase 3, antitumor efficacy, biodistribution



## INTRODUCTION

Docetaxel (DCX) is a second generation taxane, derived from the inactive 10-deacetyl baccatin III, extracted from the European Yew tree (*Taxus baccata*).<sup>1,2</sup> DCX has better water solubility, pharmacokinetic profile, and anticancer activity than paclitaxel.<sup>1,3</sup> Current FDA approved DCX products, including Taxotere, are essentially Tween 80/ethanol-based solutions,<sup>4</sup> which unfortunately are associated with various significant side effects. They induce marked hypersensitivity, neutropenia, fluid retention, and alopecia.<sup>4–6</sup> Hypersensitivity reactions, which are attributed to the Tween 80 in the formulations, can vary from simple skin rash to systemic anaphylaxis<sup>4,7</sup> and necessitate premedication with corticosteroids.<sup>8</sup> Other problems associated with the Tween 80/ethanol-based DCX formulations include the nonspecific accumulation of DCX in healthy organs, which may lead to systemic toxicity and subsequent discontinuation of therapy.<sup>9</sup>

Nanoparticle-based, Tween 80-free DCX formulations are expected to not only avoid Tween 80-related side effects but also increase the concentration of DCX in tumors due to the enhanced permeation and retention (EPR) effect.<sup>4,9,10</sup> Data from many previous studies demonstrate that nanoparticles of 100–200 nm are most successful in tumor vasculature extravasation,<sup>11,12</sup> although there are disagreements in the literature.<sup>10,13–17</sup> The heterogeneous nature of tumor type, size, location, and metastasis may contribute to the disagreements.<sup>18</sup>

In order to improve the EPR-related nanoparticles extravasation, nanoparticles should be designed to circulate longer in the blood, while the drug of interest is retained within the nanoparticles.<sup>19</sup> PEGylation is a strategy to render the surface of nanoparticles hydrophilic, thus enabling the nanoparticles to evade early opsonization and circulate longer in the blood.<sup>20,21</sup> On the other hand, for a drug to be retained within the nanoparticles, a strong affinity between the drug and the excipient(s) used to prepare the nanoparticles is required.<sup>19</sup>

Solid lipid nanoparticles (SLNs) have been extensively investigated as drug carriers.<sup>22–25</sup> Advantages of such nanocarriers include high compatibility with lipophilic drugs, ease of fabrication, and controlled release.<sup>19,22,25,26</sup> Various SLN formulations of taxanes have been previously reported.<sup>27–30</sup> Heurtault et al. reported the development of a PEGylated lipid nanocapsule formulation (LNC) for paclitaxel using a novel phase inversion-based method.<sup>31</sup> The resultant LNCs were made of an oily medium-chain triglyceride core and stabilized with soybean lecithin as a lipophilic surfactant, and PEG hydroxystearate (Solutol) as a hydrophilic surfactant.<sup>31–33</sup> Lee et al. applied a high pressure homogenization technique to

**Received:** November 18, 2013

**Revised:** January 29, 2014

**Accepted:** February 27, 2014

**Published:** March 12, 2014

prepare a SLN formulation of paclitaxel using triglyceryl myristate (trimyrustin) and phospholipids.<sup>30</sup> The formulation showed improved *in vitro* activity,<sup>30</sup> but the *in vivo* circulation time and biodistribution profile were not improved, as compared to the market product Taxol.<sup>34</sup> Videira et al. applied a factorial design to optimize formulation parameters to prepare paclitaxel SLN formulations using Compritol 888 ATO (a mixture of mono-, di-, and triglycerides of behenic acid) and Precirol AT05 (i.e., glyceryl palmito-stearate), and the final optimized formulation demonstrated an improved *in vitro* cytotoxic activity against the murine breast cancer cell line MXT-B2.<sup>35</sup>

The present study aimed at the rational selection of a triglyceride from a list of medium- and long-chain triglycerides for the development of a SLN formulation to ultimately improve the antitumor activity of DCX. Previously it was reported that low melting point triglycerides are excellent solubilizers for DCX,<sup>36</sup> prompting us to hypothesize that high melting point triglycerides will be suitable excipients for preparing DCX-incorporated SLNs. Triglycerides that are solid at body temperature were selected to ensure formulation stability and to avoid droplet coalescence.<sup>30</sup> An oil-in-water (O/W) emulsion-based method was applied, where DCX and all lipid components were dissolved in the oil phase, and the aqueous phase consisted of a 0.1% (w/v) Poloxamer 188 aqueous solution. Finally, the *in vitro* and *in vivo* antitumor activities of the selected formulation were evaluated.

## MATERIALS AND METHODS

**Materials.** DCX was from LC Laboratories (Woburn, MA, USA). The 1,2-dioleoyl-*sn*-glycero-3-phosphoethanolamine-*N*-[methoxy (polyethylene glycol)-2000] (DOPE-PEG-2000) and phosphatidylcholine from chicken egg (ePC) were from Avanti Polar Lipids, Inc. (Alabaster, AL, USA). Sepharose 4B, MTT (3-(4,5-dimethylthiazol-2-yl)-2,5-diphenyltetrazolium bromide) kit, Tween 80 (T80), Poloxamer 188 (Pluronic F68), trimyrustin (TM), trilaurin (TL), tristearin (TS), tripalmitin (TP), mannitol, sucrose, phosphate buffer saline (PBS, pH 7.4), triglyceride assay kit, and caspase 3 assay kit were all from Sigma-Aldrich (St. Louis, MO, USA). Float-A-Lyzer dialysis tubes (MWCO 50,000) were from Spectrum Chemicals & Laboratory Products (New Brunswick, NJ, USA).

**Cell Lines and Animals.** TC-1 cells (murine lung cancer cell line) were from the American Type Culture Collection (ATCC, Rockville, MD, USA) and grown in RPMI 1640, supplemented with 10% fetal bovine serum (FBS) and 1% of 100 µg/mL streptomycin and 100 IU/mL penicillin (1% P/S). M-Wnt cells (murine mammary gland cell lines) were from Dr. Stephen D. Hursting's lab at The University of Texas at Austin. M-Wnt cells were grown in a similar medium as TC-1, with an additional supplement of 1% Glutamax. Human breast adenocarcinoma cells (MDA-MB-231) were from ATCC and grown in DMEM supplemented with 5% FBS and 1% P/S. All cell culture reagents were from Invitrogen (Life Technologies, Carlsbad, CA, USA). Female C57BL/6 mice (6–8 weeks old) were from Charles River Laboratories (Wilmington, MA, USA).

**Preparation of SLNs.** SLNs were prepared using a modified emulsion/solvent evaporation method. Briefly, 1 mL of dichloromethane (DCM) containing DCX, a triglyceride (TM, TP, TL, or TS), egg PC, and DOPE-PEG-2000 in a weight ratio of 1:20:10:2 was added to 10 mL of 0.1% Poloxamer 188 aqueous solution in a glass vial, and the mixture was sonicated using a probe sonicator, with a microprobe

attached, for 40 s, at a sonication intensity of 50% (Q-sonica LLC, Newtown, CT, USA). The glass vial was placed in an ice bath during sonication to prevent heat accumulation. The emulsion was stirred for 15 min at 400 rpm in a water bath (65 °C) to evaporate DCM, and was then stirred for an additional hour at room temperature. The resultant nanoparticle suspension was concentrated to 1 mL by ultrafiltration using an Amicon device (Millipore Inc., 30,000 MWCO) (490g, 25 min, 4 °C) as previously reported.<sup>37</sup> Finally, SLNs were briefly sonicated to eliminate aggregates due to the concentrating process. DCX-free SLNs were prepared similarly without the addition of DCX. For SLNs that were used in animal studies, the ultrafiltration period was extended to 60 min to further concentrate the suspension. The prolonged ultrafiltration did not result in any significant particle size change (data not shown). SLNs were lyophilized using a Freezone freeze-dryer (Labconco Corp., Kansas City, MO, USA) with 9.25% (w/v) sucrose as a cryoprotectant. The Tween 80/ethanol-based DCX formulation (DCX in T80/E) was prepared by dissolving DCX in Tween 80 (20 mg/mL). This concentrate was then diluted with water/ethanol solution to make a final DCX solution of 4 mg/mL. The final concentrations of Tween 80 and ethanol in the solution were 20% (v/v) and 13% (v/v), respectively.

### Determination of Particle Size and Zeta Potential.

Particle size and zeta potential of the SLNs were measured using a Malvern Zetasizer Nano ZS (Malvern Instruments, Worcestershire, U.K.). Briefly, 20 µL of the concentrated SLNs in suspension were diluted to 1 mL with water, and the particle size and zeta potential were determined at room temperature.

**Transmission Electron Microscopy (TEM).** The SLNs were examined using an FEI Tecnai Transmission Electron Microscope (FEI Corporate, Hillsboro, OR, USA) at the Institute for Cellular and Molecular Biology, Microscopy and Imaging Facility at The University of Texas at Austin as previously reported.<sup>38</sup>

**Determination of DCX Content and Loading Percentage in the SLNs.** The content of DCX in the SLNs was determined using HPLC after extraction as previously reported with modifications.<sup>30</sup> Briefly, SLNs in suspension were diluted 5–10 times with methanol in a glass vial, which was placed in a water bath (65 °C) for 20 min to dissolve the lipids, and placed at –20 °C for 45 min. The supernatant was collected by centrifugation at 18000g for 10 min at 4 °C (Beckman Coulter Inc., Brea, CA, USA), and 5 µL of the supernatant was used for HPLC assay as previously described.<sup>39</sup> The HPLC system consisted of an Agilent HPLC workstation (Agilent Corp., Santa Clara, CA, USA), with RP-C18 column (Zorbax Eclipse, 5 µm, 4.6 mm × 150 mm; Santa Clara, CA, USA). The mobile phase was acetonitrile and water (1:1, v/v). The flow rate was 1 mL/min, and the detection wavelength was 230 nm. The DCX loading percentage was measured using a similar procedure, with the exception that the SLNs were lyophilized, and 5 mL of methanol was added to 5 mg of the lyophilized SLNs. The weight percentage of DCX in the SLNs (% w/w) was calculated based on the following formula:<sup>40</sup>

$$\text{drug loading \%} = \frac{\text{DCX weight (mg)}}{\text{SLN weight (mg)}} \times 100$$

**Gel Permeation Chromatography (GPC).** To investigate whether free DCX coexisted with DCX-SLNs in the nanoparticle preparation, the SLNs (100 µL) were applied to a

Sephacose 4B column (6 mm × 30 cm) equilibrated with water, and the DCX-SLNs were eluted with water. Fractions of 0.5 mL were collected, and 0.3 mL of each fraction was lyophilized to determine the content of DCX as mentioned above. In addition, the absorbance of each fraction (100  $\mu$ L) at 500 nm was measured using a BioTek Synergy HT Multi-Mode Microplate Reader (Winooski, VT, USA) to determine their turbidity, which was used as an indication of the presence of nanoparticles in the fractions collected. Finally, the concentration of triglycerides in each fraction was also measured using a Sigma Triglyceride Assay Kit following the manufacturer's instruction.

**Short-Term Stability Study.** DCX-SLNs prepared using different triglycerides were stored in PARAFILM-sealed vials at 4 °C for eight days. Particle size, zeta potential, and DCX content were measured as mentioned above shortly after the preparation and on day 8 to monitor any change of these parameters.

**In Vitro Release of DCX from the SLNs.** The release of DCX from the SLNs made with different triglycerides was monitored using Float-A-Lyzer tubes (MWCO 50,000). Briefly, DCX-SLNs suspension was diluted to 1 mL with PBS and transferred to the dialysis tube, which was then placed in a 50 mL plastic tube containing 20 mL of release medium (PBS, 0.1 mM, pH7.4, with 1% Tween 80). The tubes were then placed at 37 °C in an orbital shaker at 100 rpm (Max-Q 5000, Thermo Scientific, Waltham, MA, USA). At predetermined time points, the whole release medium was replaced with fresh medium to maintain sink condition, and DCX concentration was analyzed using HPLC as previously mentioned. The release of DCX from the DCX in T80/E formulation was evaluated similarly for comparison.

**Modulated Differential Scanning Calorimetry (mDSC).** For mDSC, a TA Instruments model 2920 DSC (New Castle, DE, USA) was used, and the data were analyzed using TA Universal Analysis 2000 software. Accurately weighed samples were placed in aluminum crimped pans. The ramp rate was 5 °C/min, and the temperature range was from 10 to 200 °C. The modulation amplitude and period were 0.5 °C and 40 s, respectively. Ultrahigh purity nitrogen was flowing through the sample chamber during the run. Samples included DCX, trimyristin, DCX-SLNs (prepared with trimyristin), blank SLNs, and the physical mixture of DCX and blank SLNs.

**X-ray Diffraction (XRD).** A Philips model 1710 X-ray diffractometer (Philips Electronic Instruments Inc., Mahwah, NJ, USA) available in the Texas Materials Institute X-ray Facility at The University of Texas at Austin was used to analyze the crystallinity of DCX in the SLNs. Samples included DCX alone, DCX-SLNs (prepared with trimyristin), DCX mixed with blank SLNs, and blank SLNs.

**Cell Proliferation Assay.** Cells were seeded in 96-well plates at a density of 3,000 cells/well and incubated at 37 °C with 5% CO<sub>2</sub> overnight. They were treated with various concentrations of DCX-SLNs (prepared with trimyristin), DCX in T80/E, blank SLNs, or T80/E alone for 72 h. Cell viability was determined using an MTT assay as previously described.<sup>39</sup> IC<sub>50</sub> values were calculated using GraphPad prism (GraphPad software, Inc., La Jolla, CA, USA).

**Caspase 3 Activity Assay.** Caspase 3 activity was determined using a Sigma-Aldrich Caspase 3 Fluorimetric Assay Kit. In brief, TC-1 cells were seeded in 24-well plates at 25,000 cells/well and incubated overnight. The cells were treated with DCX-SLNs (prepared with trimyristin), DCX in

T80/E, blank SLNs, or T80/E for 72 h. The concentration of the DCX was 0.01  $\mu$ M. The cells were then washed with PBS and lysed. The cell lysate was centrifuged at 18000g for 10 min at 4 °C. The supernatant was transferred to a clear-bottomed black plate and mixed with the assay substrate, acetyl-Asp-Glu-Val-Asp-7-amido-4-methylcoumarin (Ac-DEVD-AMC). The mixture was incubated for 6 h for the hydrolysis of the Ac-DEVD-AMC by caspase 3 to release the fluorescent AMC, which was quantified by measuring the fluorescence intensity at 360 nm (excitation)/460 nm (emission) according to the manufacturer's instruction. The unit of the caspase 3 activity was mol AMC/min/mL. A caspase 3 inhibitor (provided in the kit) was used to confirm that the fluorescence was due to caspase 3 activity. Total protein concentration in the cell lysates was determined using Bio-Rad DC Protein Assay Kit following the manufacturer's instruction.

**Evaluation of the Antitumor Activity of the DCX-SLNs in Vivo.** All animal protocols were approved by the Institutional Animal Care and Use Committee at the University of Texas at Austin, and the National Institutes of Health (NIH) guidelines for laboratory animal use and care were followed. Animals were left to acclimatize for at least 7 days upon arrival from the vendor. Each mouse was injected with the murine TC-1 lung cancer cells ( $5 \times 10^5$  cells per mouse) suspended in 100  $\mu$ L of FBS-free RPMI 1640 medium subcutaneously in the shaved left flank. Six days after the implantation (day 6), mice were randomized into 4 groups, 7 mice per group, and injected intravenously via the tail vein with DCX-SLNs (prepared with trimyristin), DCX in T80/E, blank SLNs, or 5% mannitol as a vehicle control. The dose of DCX was 15 mg/kg body weight. Mannitol was used to adjust the tonicity of the nanoparticle suspension. Injection was repeated on days 9 and 12 postimplantation. Tumor sizes were measured using a digital caliper, and tumor volumes were calculated using the following formula:<sup>41</sup>

$$\begin{aligned} \text{tumor volume (mm}^3\text{)} \\ = [\text{length (mm)} \times \text{width (mm)} \times \text{width (mm)}] \times 0.5 \end{aligned}$$

On day 21, mice were euthanized to harvest tumor tissues, which were weighed, fixed in Zn formalin buffer for immunohistochemistry.

**Immunohistochemistry.** Tissue sample preparation for immunohistochemical evaluation was carried out in the Histology and Tissue Analysis Core at Dell Pediatric Research Institute (DPRI) at The University of Texas at Austin. The formalin-fixed tumor tissues were embedded in paraffin wax, sectioned, and stained with an antibody against CD-31 (Abcam, Cambridge, MA, USA) as a marker for angiogenesis ( $n = 3$ ).<sup>41</sup> Slides were then scanned, and images were taken using the ScanScope XT (Aperio Technologies, Vista, CA, USA).

**Biodistribution and Tumor Uptake.** TC-1 tumors were implanted in female C57BL/6 mice as mentioned above. Three weeks after tumor implantation, mice were divided into 2 groups ( $n = 9-10$ ); one group was injected with DCX in T80/E (equivalent to DCX dose of 16 mg/kg) via the tail vein, and the other group with DCX-SLNs prepared with trimyristin (equivalent to DCX dose of 16 mg/kg). Two or twelve hours later, 4-5 mice from each group were euthanized to collect tumor, liver, kidney, spleen, heart, lung, and blood samples. The organs and tumor tissues were weighed and then stored at -80 °C. The blood samples were mixed with an EDTA solution and allowed to stand for about 15 min and centrifuged (3300g, 10

Table 1. Physical Parameters of DCX-SLNs Prepared with Different Triglycerides<sup>a</sup>

SLNs	triglyceride	particle size (nm)	polydispersity index	zeta potential (mV)	DCX loading (% w/w)
TS	tristearin	178.4 ± 2.3	0.181	-29.6 ± 2.3	2.6 ± 0.2
TP	tripalmitin	176.3 ± 3.9	0.162	-30.7 ± 2.8	2.8 ± 0.1
TM	trimyristin	182.8 ± 2.0	0.196	-29.8 ± 1.8	2.4 ± 0.1
TL	trilaurin	150.7 ± 14.5	0.165	-29.3 ± 1.5	2.5 ± 0.1

<sup>a</sup>Data shown are mean ± SD (*n* = 3).

min, 4 °C) to separate the plasma, which was stored at -80 °C. DCX was extracted from the samples using ethyl acetate, and DCX concentrations in the samples were determined using HPLC. Paclitaxel was used as an internal standard.

**Statistical Analyses.** Statistical analyses were completed by performing ANOVA followed by Fisher's protected least significant difference procedure. A *p*-value of ≤0.05 (two-tail) was considered significant.

## RESULTS

**Preparation of DCX-SLNs and Selection of Triglyceride in the SLNs.** SLNs were prepared using a modified emulsion/solvent evaporation method. The nanoparticles were composed of DCX, a triglyceride, ePC, DOPE-PEG-2000, and Pluronic F68. The average particle size of SLNs produced using tristearin, tripalmitin, trimyristin, and trilaurin as the triglyceride was 178.4 ± 2.3, 176.3 ± 3.9, 182.8 ± 2.0, and 150.7 ± 14.5 nm, respectively (Table 1). The polydispersity indices of all nanoparticle preparations were equal to, or below, 0.2. The zeta potential of the SLNs was approximately -30 mV. The content of DCX in the final SLNs was 2.4–2.8% (w/w) (Table 1).

The release profiles of DCX are shown in Figure 1. The release of DCX from the SLNs was slower, relative to the diffusion of DCX out of the DCX in T80/E formulation (Figure 1A). Only about 4.5–9% of the DCX was released from the SLN formulation within the first 6 h, whereas about 31% of DCX diffused out of the T80/E formulation within the same time period (Figure 1A). The rate at which the DCX was released from the DCX-SLNs prepared with trimyristin was the slowest (Figure 1B).

During a short-term, 8-day stability study at 4 °C, no significant change in particle size and DCX content in any of the four DCX-SLNs preparations was found (Figures 2A,B). However, the zeta potential of DCX-SLNs prepared with tripalmitin and trilaurin changed significantly (Figure 2C). Based on data shown in Figures 1 and 2, the DCX-SLNs prepared with trimyristin were chosen for further studies, because the release of DCX from the SLNs prepared with trimyristin was the slowest, and the resultant DCX-SLNs were also relatively more stable.

**Characterization of DCX-SLNs Prepared with Trimyristin as the Triglyceride.** Shown in Figure 3A are the GPC results for the DCX-SLNs prepared with trimyristin as the triglyceride. About 90% of the DCX that was eluted from the column was associated with the triglyceride and with the fractions that contained the nanoparticles (calculated based on the area under curves of the GPC profiles) (Figure 3A). TEM showed that the DCX-SLNs are spherical (Figure 3B). The SLNs were successfully lyophilized with 9.25% (w/v) sucrose as a cryoprotectant (data not shown).

DSC analysis of the DCX-SLNs, free DCX, blank SLNs, and blank SLNs mixed with DCX showed that DCX exhibited a characteristic melting peak at 167.4 °C (Figure 4A). The physical mixture exhibited an endothermic melting peak at

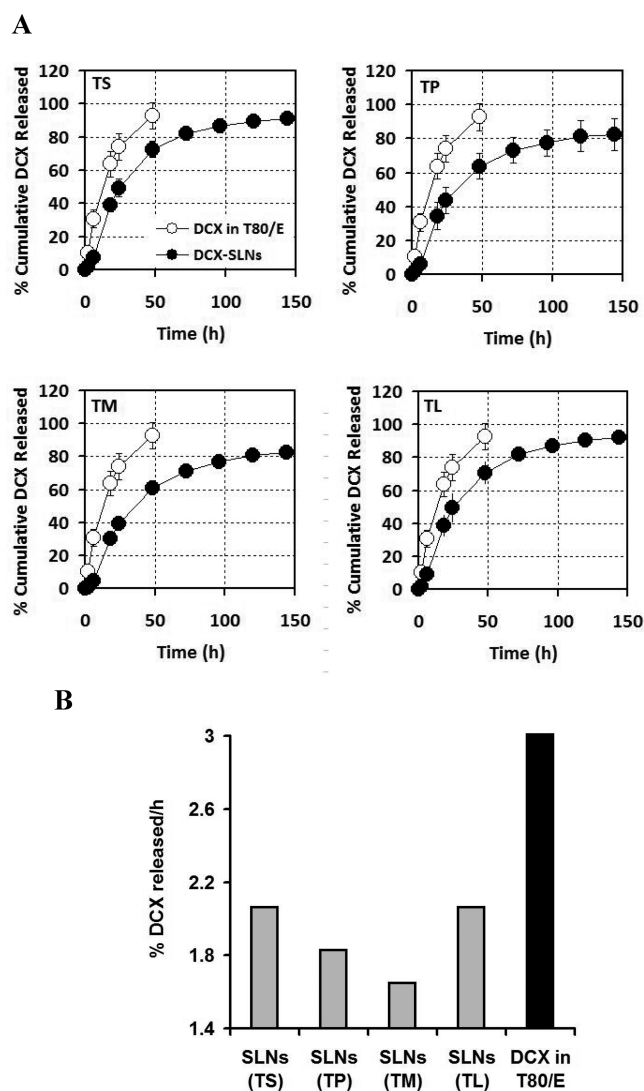


**Figure 1.** (A) The release of DCX from DCX-SLNs (closed circles) prepared using tristearin (TS), tripalmitin (TP), trimyristin (TM), or trilaurin (TL). As a control, the release of DCX from DCX in T80/E (open circles) was also included. Each point represents mean ± SD from three independent measurements. (B) A comparison of the percent of DCX released per hour from DCX-SLNs prepared using different triglycerides. The release rates were calculated with data in the initial 24 h period. Each point represents mean (*n* = 3).

143.4 °C, which can be attributed to the presence of free DCX, as the blank SLNs did not show any distinct peak at that temperature. A distinct DCX endothermic melting peak was also absent in the DCX-SLNs (Figure 4A). On the other hand, the presence of the endothermic melting peak of trimyristin at approximately 55–58 °C confirmed the solid state of the lipid within the SLNs (Figure 4A). Finally, XRD showed that a

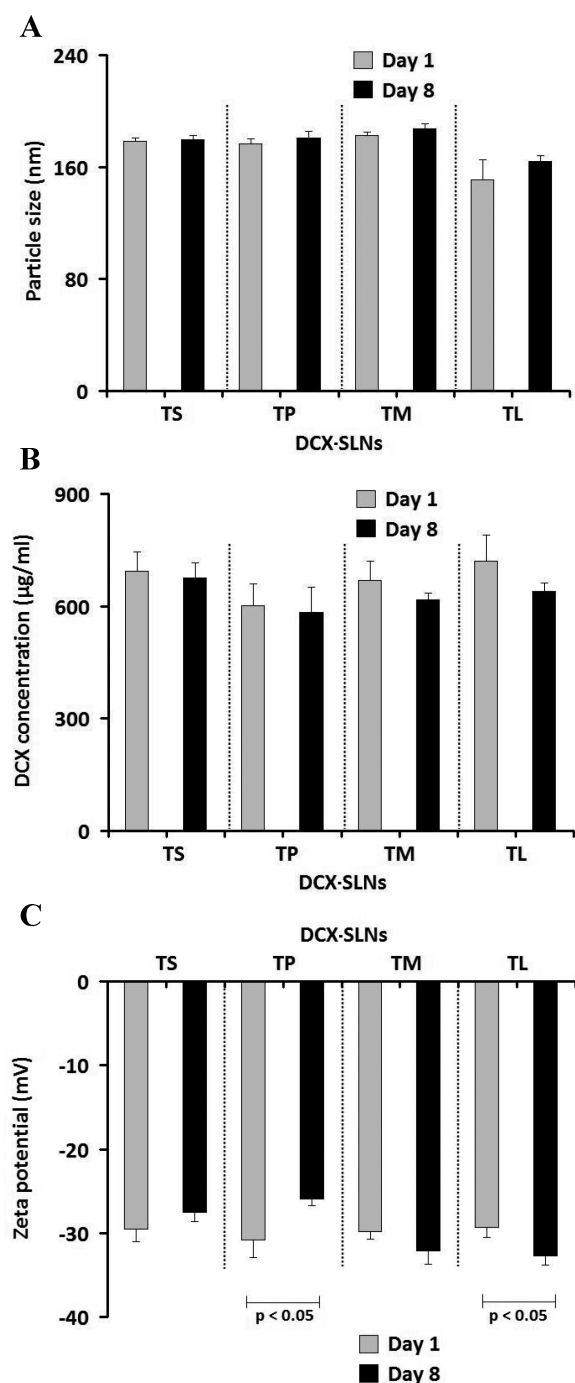


**Figure 2.** The particle sizes (A), DCX contents (B), and zeta potentials (C) of DCX-SLNs prepared with different triglycerides shortly after preparation or after 8 days of storage at 4 °C. Data shown are mean  $\pm$  SD ( $n = 3$ ).

characteristic DCX peak was present in the physical mixture, but absent from the DCX-SLN composition (Figure 4B).

**Cytotoxicity of the DCX-SLNs Prepared with Trimyrustin as a Triglyceride against Tumor Cells in Culture.** MTT assay revealed that both DCX-SLNs and DCX in T80/E inhibited the proliferation of tumor cells, including murine mammary gland cancer cells (M-Wnt), murine lung cancer cells (TC-1), and human breast adenocarcinoma cells (MDA-MB-231). However, the  $\text{IC}_{50}$  values of the DCX-SLNs were significantly lower than that of the DCX in T80/E in each of

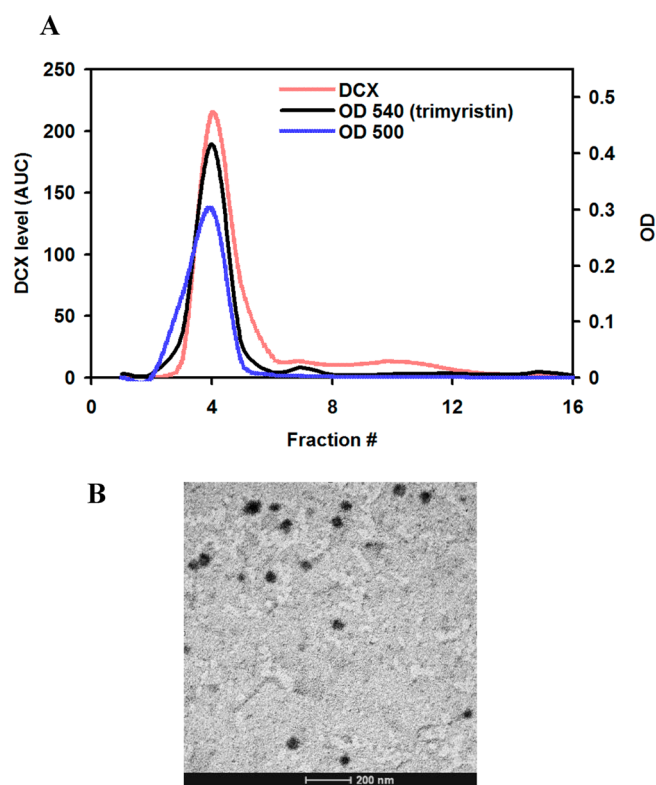


**Figure 3.** (A) A representative GPC profile of DCX-SLNs prepared with trimyrustin. Collected fractions were divided into three portions: one was analyzed for DCX content (red), one was used to measure turbidity (OD 500 nm) (blue), and the other one was used to measure trimyrustin concentrations, and the visible absorbance of the formed colored component was measured (OD 540) (black). This experiment was repeated three times with similar results. (B) A representative TEM image of DCX-SLNs prepared with trimyrustin (bar =200 nm).

the three cell lines (Figure 5A). At the highest equivalent DCX concentrations tested (i.e., 0.01, 1, and 0.05  $\mu\text{M}$  in M-Wnt, TC-1, and MDA-MB-231, respectively), both the blank SLNs and the T80/E vehicle control did not show any significant toxicity in all three cell lines (data not shown).

Caspase 3 activity was also measured in TC-1 cells treated with DCX-SLNs, DCX in T80/E, blank SLNs, and T80/E at a DCX concentration of 0.01  $\mu\text{M}$ . Caspase 3 activity in cells treated with the DCX-SLNs was significantly higher than in cells treated with DCX in T80/E ( $p < 0.005$ , Figure 5B). The total protein contents in the cell lysates in all four groups were not significantly different (data not shown).

**The Antitumor Activity of the DCX-SLNs Prepared with Trimyrustin as a Triglyceride in a Mouse Model.** The antitumor activity of DCX-SLNs was evaluated in TC-1 murine lung cancer model pre-established in C57BL/6 mice. As shown in Figure 6A, both DCX-SLNs and DCX in T80/E significantly inhibited the growth of the TC-1 tumors in mice. However, the DCX-SLNs were significantly more effective than the DCX in T80/E formulation, starting on day 15 (Figure 6A). The average body weights of mice that were injected with blank SLNs or 5% mannitol (as a vehicle control) increased slightly ( $\sim 10\%$ ) during the 21 days after tumor cell implantation, while the average body weight of mice that were treated with DCX-SLNs or DCX in T80/E did not show any significant change (Figure 6B). Finally, the average weight of tumors in mice that were treated with the DCX-SLNs was also significantly lower

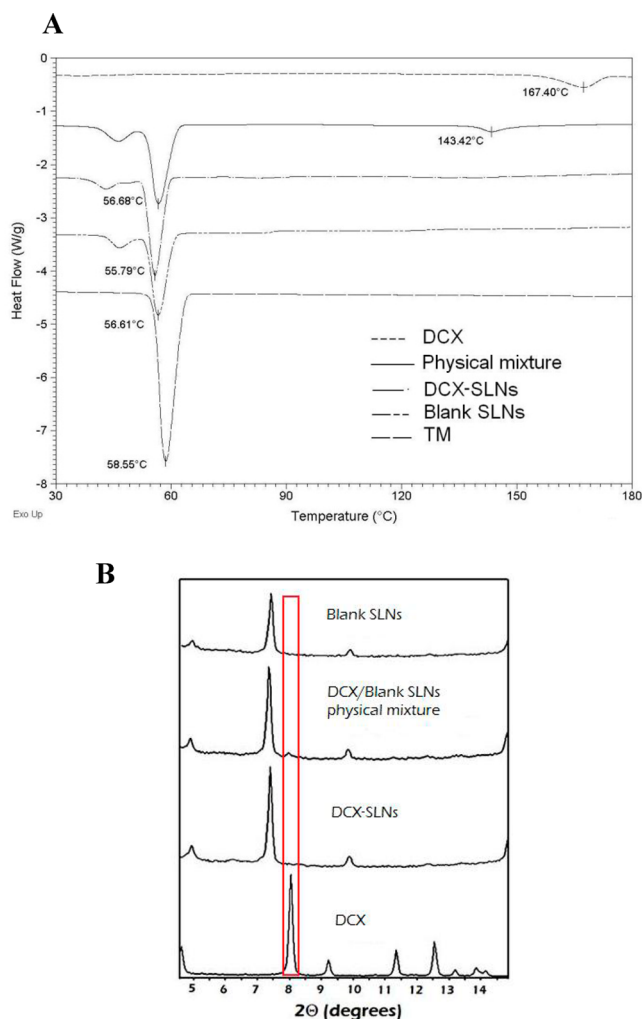


**Figure 4.** DSC thermograms (A) and X-ray diffractograms (B) of DCX-SLNs, DCX alone, trimyristin (TM) alone, blank SLNs, or the physical mixture of blank SLNs and DCX.

than that in other groups at the end of the study (Figure 6C). Anti-CD31 staining (i.e., angiogenesis marker) showed that the extent of CD31<sup>+</sup> staining tended to be lower in tumors in mice that were treated with the DCX-SLNs, as compared to in other groups (Figure 6D).

**Biodistribution Study.** Figure 7 shows the concentration of DCX in tumors and other organs in TC-1 tumor-bearing mice 2 and 12 h after the mice were injected intravenously with either DCX-SLNs (prepared with trimyristin) or DCX in T80/ethanol. The concentration of DCX in tumors in mice that were injected with DCX-SLNs was about 50% higher than in mice that were injected with the DCX in T80/ethanol formulation, 12 h after the injection ( $p < 0.05$ ) (Figure 7A). However, the concentration of DCX in the liver, spleen, kidneys, heart, and lungs of mice that were injected with the DCX-SLNs were lower than in mice that were injected with the DCX in T80/E formulation (Figures 7B–F). Finally, 2 h after intravenous injection, the concentration of DCX in the plasma in mice that were injected with the DCX-SLNs was about 5-times higher than in mice that were injected with the DCX in T80/E formulation (Figure 7G).

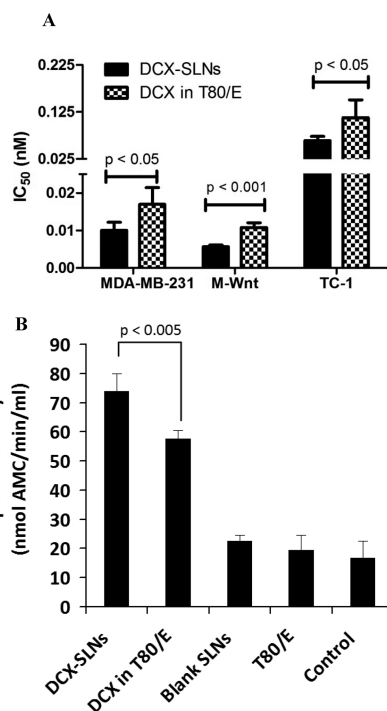


**Figure 5.** (A) The IC<sub>50</sub> values of DCX-SLNs and DCX in T80/E in MDA-MB-231, M-Wnt, and TC-1 cells. Cells were incubated with the DCX formulations for 72 h. (B) Caspase 3 activity (in nmol AMC/min/ml) in TC-1 cells following 72 h of incubation with DCX-SLNs or DCX in T80/E (DCX, 0.01 μM). Controls include blank SLNs, T80/E vehicle, or medium alone. Data shown are mean ± SD ( $n = 4$ ).

## DISCUSSION

Since the discovery of taxanes in the mid-1980s, the fervent search for more efficacious and less toxic taxane formulations has led to the FDA approval of three market products, namely, Taxol (Bristol-Myers Squibb, Princeton, NJ, USA), Taxotere (Sanofi-Aventis U.S. LLC, Bridgewater, NJ, USA), and Abraxane (Celgene Corporation, Summit, NJ, USA). In addition, a polymeric PEGylated micelle formulation of paclitaxel (Genexol-PM) has been marketed in South Korea since 2007,<sup>42–44</sup> and others (e.g., BIND-014) are in the pipeline.<sup>44</sup> Taxotere used to be the only FDA-approved DCX formulation on the U.S. market. Generic DCX products that are currently in the U.S. include formulations launched by Hospira, Sagent, and Accord, which are all DCX in Tween 80/ethanol solutions. Docefrez is a lyophilized DCX powder to be reconstituted with 3.54% ethanol in Tween 80 before injection. DCX has low water solubility ( $\sim 5 \mu\text{g/mL}$ ),<sup>45</sup> and Tween 80 and ethanol are used in the current DCX formulations to solubilize DCX.

The main aim in the present study was to rationally design a Tween 80-free formulation of DCX that also improves the antitumor activity of DCX. Based on a study by Huynh et al., where the authors reported that DCX solubility in low melting point triglycerides, such as tributyrin, tricaproin, and tricaprylin, is 10,000–20,000 times more than in water,<sup>36</sup> we postulated that triglyceride-based SLN formulations may exhibit attractive drug–excipient interaction, facilitating incorporation of DCX in the nanoparticles. Four different medium- and long-chain saturated triglycerides that are solid at body temperature were employed in this study; namely, trilaurin (mp 46 °C), trimyristin (mp 57 °C), tripalmitin, (mp 66 °C), and tristearin

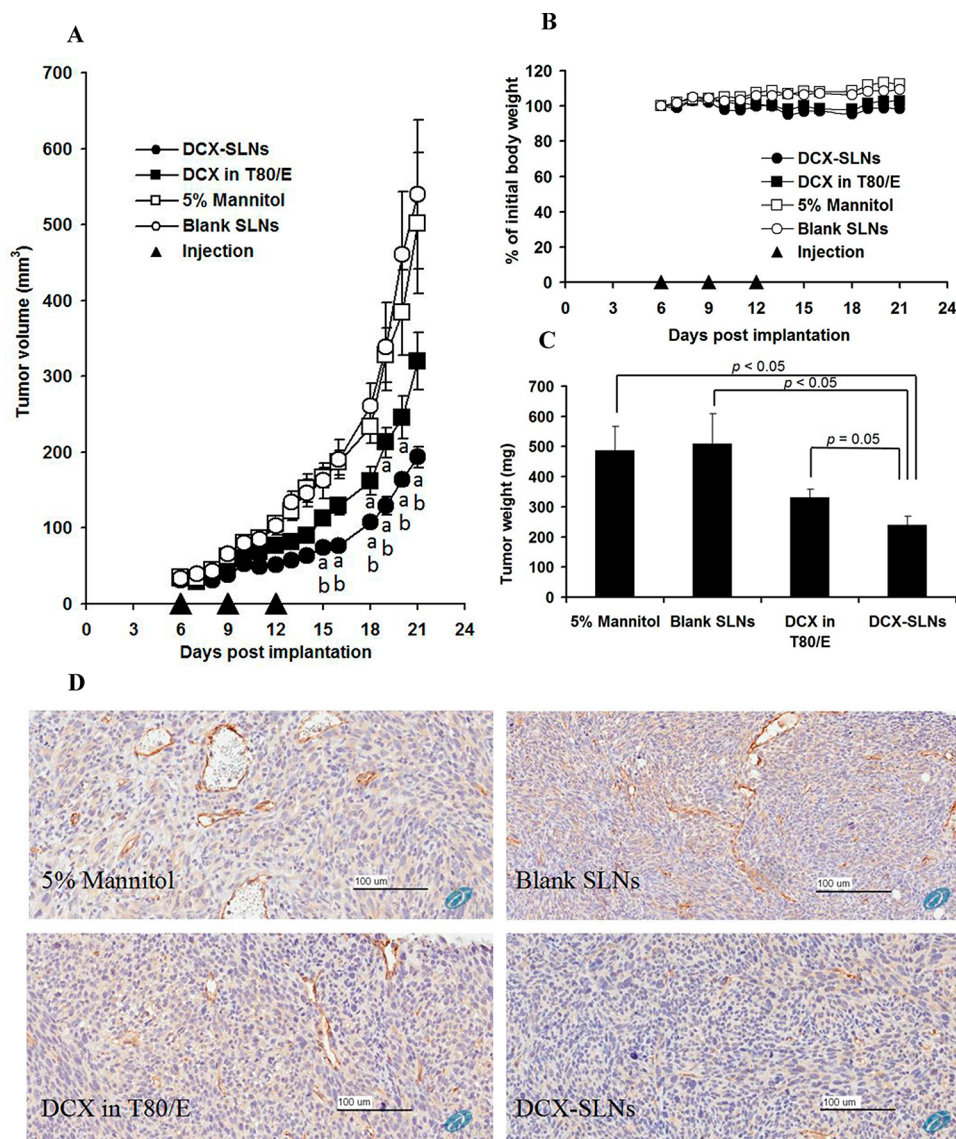


**Figure 6.** (A) The growth curves of TC-1 tumors in C57BL/6 mice (<sup>a</sup> $p < 0.05$ , DCX-SLNs or DCX in T80/E vs 5% mannitol, <sup>b</sup> $p < 0.05$ , DCX-SLNs vs DCX in T80/E). (B) The changes in the body weight of TC-1 tumor-bearing mice. (C) The weights of tumors at the end of the study. (D) Representative images of tumor tissues after anti-CD31 staining (bar = 100 μm). Mice were iv injected with DCX-SLNs or DCX in T80/E at a DCX dose of 15 mg/kg via the tail vein on days 6, 9, and 12 after tumor implantation. Controls included mice that were injected with blank SLNs or 5% mannitol. Data shown in A–C are mean  $\pm$  SEM ( $n = 7$ ).

(mp 69 °C) with fatty acid chain lengths of 12 (C12:0), 14 (C14:0), 16 (C16:0), and 18 (C18:0) carbon atoms, respectively. It was reported that triglycerides with melting points lower than room temperature form nanodroplets that are prone to coalescence during preparation or storage.<sup>29,30</sup> The use of high melting point triglycerides may significantly decrease the mobility of the drug molecules within the lipid core and thus reduce immature drug leakage.<sup>30,34</sup>

Therefore, tricaprylin (C8:0, mp 9 °C), tricaprln (C10:0, mp 31 °C), and trolein (C18:1, mp 5 °C) were excluded. The trimyristin-based SLN formulation was chosen from the four tested formulations because the rate at which the DCX was released from them was the slowest (Figure 1), and the SLNs were also more stable (Figure 2). In a mouse model with pre-established TC-1 mouse tumors, the DCX-SLNs were significantly more effective than DCX in T80/E in inhibiting the tumor growth (Figure 6), likely because the DCX-SLNs significantly increased the accumulation of DCX in tumor

tissues (Figure 7A). Circulating nanocarriers usually take advantage of the leaky vasculature and/or poor lymphatic drainage in tumor tissues to accumulate in tumors.<sup>17,46</sup> Since DCX accumulation in tumor was only significantly higher at 12 h, but not at 2 h, following the administration of SLNs, as compared to the DCX in T80/E, it is likely that the enhanced retention of the DCX-SLNs in tumors due to poor lymphatic drainage was responsible for the improved accumulation.<sup>17,18</sup> Small molecules may also exhibit enhanced permeation to tumors as well due to the leaky neovasculature in the tumor tissues, however, they can easily diffuse out of tumors as well, while macromolecules and nanocarriers are entrapped and consequently accumulate.<sup>47–49</sup>

DCX not only induces apoptosis due to microtubule assembly stabilization, but also is antiangiogenic.<sup>3,50</sup> Inhibition of the formation of new blood vessels that provide rapidly growing tumors with increasing nutritional demand is expected to stunt the tumor growth.<sup>9,10,16</sup> Furthermore, the hastily

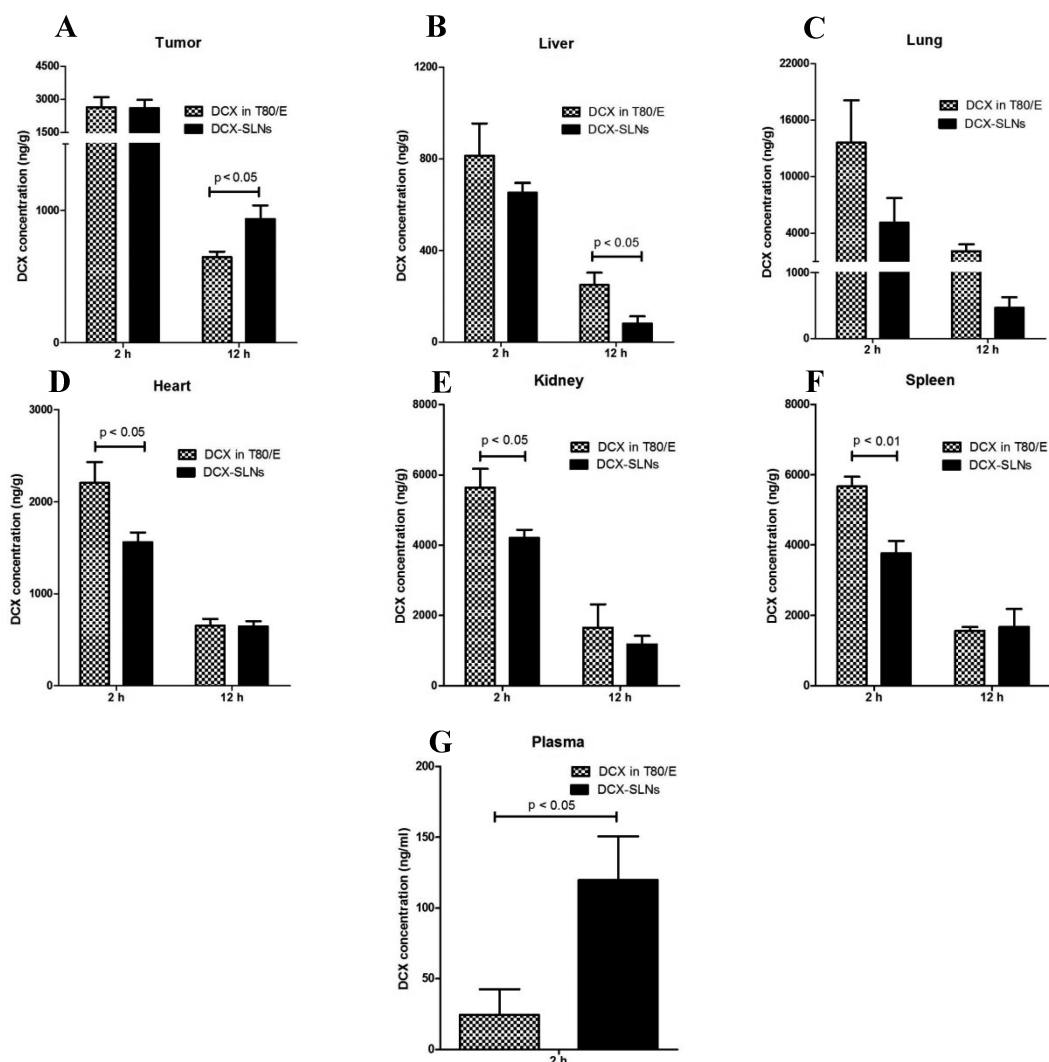


**Figure 7.** The concentrations of DCX in tumor (A), liver (B), lungs (C), heart (D), kidneys (E), spleen (F), and plasma (G) of TC-1 tumor-bearing C57BL/6 mice 2 or 12 h after iv injection of either DCX-SLNs or DCX in T80/E. The dose of DCX was 16 mg/kg. Data shown are mean  $\pm$  SEM ( $n = 4-5$ ).

formed tumor-associated vasculature is characterized with various fenestration and imperfections, and almost lacking any intact lymphatic drainage.<sup>17,18,48,51</sup> Nanoparticles are known to take advantage of this leaky tumor vasculature to extravasate into the tumor microenvironment, where they can accumulate.<sup>46</sup> Several groups have reported lipid nanoparticle-based DCX formulations before.<sup>27,30,39,52-54</sup> The most widely used lipid excipients are soy lecithin, glycerides, or a mixture of the two. For example, Liu et al. formulated DCX into a nanostructured lipid carrier based on soy lecithin, glyceryl monostearate, and fatty acids,<sup>54</sup> but the DCX in nanostructured lipid carrier was only slightly more effective than a DCX in a T80/E formulation (Duopafei) against B16 tumors in mice.<sup>54</sup> Xu et al. designed a trimyristin-based SLN formulation for DCX to treat hepatocellular carcinoma.<sup>27</sup> To improve their liver uptake, the SLNs were not PEGylated. Instead, their surface was galactosylated to target asialoglycoprotein receptors overexpressed on the surface of hepatoma cell lines.<sup>27</sup>

We previously reported the formulation of DCX-loaded lecithin-based PEGylated SLNs.<sup>39</sup> The resultant SLNs showed an improved *in vitro* cytotoxic activity, in addition to improved tumor accumulation in a mouse model. However, the capacity

of this formulation in incorporating DCX was limited, which may be attributed to the limited affinity between DCX and the excipients.<sup>39</sup> In the present study, in order to rationally select the most suitable excipient, four DCX-SLN formulations were prepared using four different high melting point triglycerides.

As discussed previously, a successful formulation for taxane is the one that exhibits (a) long plasma circulation time, (b) long drug retention within the delivery carrier, which requires high drug-excipient affinity and slow release, (c) high tumor accumulation, and (d) favorable biodistribution profile, as less drug goes to healthy tissues.<sup>19</sup> Drug release behavior from the DCX-SLNs and short-term stability were the criteria for triglyceride selection in this study. In this regard, the absence of a burst release of DCX from the DCX-SLNs in the first 2 h and a subsequent slower release rate predict a limited drug leakage from the nanoparticles in the blood circulation before reaching tumors.<sup>55</sup> The release of DCX from the tristearin-based and trilaurin-based DCX-SLNs was relatively faster (Figure 1), and the tripalmitin- and trilaurin-based DCX-SLNs showed instability, as the zeta potential changed significantly following a short-term storage (Figure 2). Change in zeta potential has been used as an indicator of nanoparticle



instability.<sup>56,57</sup> Several reports indicated that trilaurin does not exist in the solid state within the SLNs, but rather as a “supercooled-liquid state” that resembles O/W emulsions, even at 4 °C, which was not the case with triglycerides having higher melting points.<sup>56,58,59</sup> The relatively faster release of DCX from the trilaurin-based SLNs may also arise as a result of the same phenomenon. As to the SLNs prepared with tripalmitin, the “supercooled liquid state” phenomenon was not reported, therefore, the reasons to which this sign of instability may be attributed need to be investigated. On the other hand, the absence of a burst release of DCX from the DCX-SLNs prepared with trimyristin may infer a strong DCX–trimyristin interaction. It was reported that the solubility of DCX in tributyrin (4 C chain) is about 108 mg/mL, and it gets lower with higher chain length, reaching about 56 mg/mL with tricaprylin (8 C chain).<sup>36</sup> Based on this, and since DSC and XRD data (Figure 4) implied that there is a strong interaction between DCX and the excipients, it is speculated that DCX exists in the SLNs in either a noncrystalline state or a dissolved state, or both, within the lipid matrix. Existence of DCX in the amorphous state within lipid-based matrices was also reported previously.<sup>60</sup> The disappearance of the characteristic DCX-related peaks in DSC and XRD was previously shown to be related to the loss of DCX crystallinity.<sup>60,61</sup> In fact, we also found that the characteristic melting peak of DCX at 167 °C completely disappeared upon analyzing the thermal behavior of DCX–trimyristin mixtures at DCX to trimyristin ratios of 1:5, 1:2, and 1:1 using DSC (data not shown), suggesting the prevalence of a strong interaction between the DCX and trimyristin. The relatively slower release of DCX from trimyristin-based DCX-SLNs may also be attributed to the strong DCX–lipid interaction as well.

Finally, potential toxicity issues were also considered during excipient selection. Long-chain triglycerides in soybean oil and egg yolk phospholipids are commonly used in intravenous fat emulsions as components of parenteral nutrition for patients who are not able to receive nutrition via oral diets (e.g., Intralipid, B Braun Medical Inc., Bethlehem, PA). Triglycerides are metabolized in the blood by lipases into corresponding fatty acids, which are cleared from the blood within about 30 min.<sup>62</sup> Phosphatidylcholine and PEGylated phosphoethanolamine are used in products that are approved for intravenous infusion in humans (e.g., Doxil). Therefore, we expect that our new DCX-SLN formulations will likely have a favorable safety profile. In fact, the body weights of the tumor-bearing mice that were treated with the DCX-SLNs did not significantly change by the end of the efficacy study (Figure 6B). In addition, the concentrations of DCX in vital organs such as liver, spleen, kidneys, lungs, and heart of mice that were injected with the DCX-SLNs were significantly lower than in mice that were injected with the DCX in T80/E formulation (Figure 7), indicating that our DCX-SLNs may be less damaging to those vital organs than Taxotere.

## CONCLUSION

In the present study, by taking advantage of the high solubility of DCX in triglycerides, we successfully prepared several DCX-incorporated SLNs using various medium- and long-chain triglycerides. The DCX-SLN composition prepared with trimyristin was selected for further evaluation because the resultant DCX-SLNs were stable in a short-term stability study, and the rate at which the DCX was released from them was the slowest. The DCX-SLNs showed a stronger antitumor activity

than DCX solubilized in a Tween 80/ethanol mixture in cell culture and, more importantly, in a mouse model with pre-established tumors, likely because the DCX-SLNs significantly increased the accumulation of the DCX in tumor tissues. The decreased accumulation of DCX in vital organs after iv injection of DCX-SLNs, relative to after injection of DCX solubilized in a Tween 80/ethanol mixture, suggests that the DCX-SLNs may have a favorable safety profile.

## AUTHOR INFORMATION

### Corresponding Author

\*The University of Texas at Austin, Dell Pediatric Research Institute, 1400 Barbara Jordan Boulevard, Austin, TX 78723. Tel: (512) 495-4758. Fax: (512) 471-7474. Email: zhengrong.cui@austin.utexas.edu.

### Notes

The authors declare no competing financial interest.

## ACKNOWLEDGMENTS

This work was supported in part by a National Cancer Institute grant (CA135274 to Z.C.) and the University of Texas at Austin, College of Pharmacy. Y.W.N. was supported by a doctoral scholarship from the Egyptian Ministry of Higher Education. The authors would like to thank Dr. Steve Swinnea in the Texas Material Institute X-Ray Facility at The University of Texas at Austin for his help with XRD.

## REFERENCES

- (1) Zhao, P.; Astruc, D. Docetaxel nanotechnology in anticancer therapy. *ChemMedChem* **2012**, *7* (6), 952–972.
- (2) Cortes, J. E.; Pazdur, R. Docetaxel. *J. Clin. Oncol.* **1995**, *13* (10), 2643–2655.
- (3) Herbst, R. S.; Khuri, F. R. Mode of action of docetaxel - a basis for combination with novel anticancer agents. *Cancer Treat. Rev.* **2003**, *29* (5), 407–415.
- (4) Engels, F. K.; Mathot, R. A.; Verweij, J. Alternative drug formulations of docetaxel: a review. *Anticancer Drugs* **2007**, *18* (2), 95–103.
- (5) Tan, Q.; Liu, X.; Fu, X.; Li, Q.; Dou, J.; Zhai, G. Current development in nanoformulations of docetaxel. *Expert Opin. Drug Delivery* **2012**, *9* (8), 975–990.
- (6) Seo, Y. G.; Kim, D. W.; Yeo, W. H.; Ramasamy, T.; Oh, Y. K.; Park, Y. J.; Kim, J. A.; Oh, D. H.; Ku, S. K.; Kim, J. K.; Yong, C. S.; Kim, J. O.; Choi, H. G. Docetaxel-loaded thermosensitive and bioadhesive nanomicelles as a rectal drug delivery system for enhanced chemotherapeutic effect. *Pharm. Res.* **2013**, *30* (7), 1860–1870.
- (7) ten Tije, A. J.; Verweij, J.; Loos, W. J.; Sparreboom, A. Pharmacological effects of formulation vehicles: implications for cancer chemotherapy. *Clin. Pharmacokinet.* **2003**, *42* (7), 665–685.
- (8) Hennenfent, K. L.; Govindan, R. Novel formulations of taxanes: a review. Old wine in a new bottle? *Ann. Oncol.* **2006**, *17* (5), 735–749.
- (9) Brannon-Peppas, L.; Blanchette, J. O. Nanoparticle and targeted systems for cancer therapy. *Adv. Drug Delivery Rev.* **2004**, *56* (11), 1649–1659.
- (10) Alexis, F.; Rhee, J. W.; Richie, J. P.; Radovic-Moreno, A. F.; Langer, R.; Farokhzad, O. C. New frontiers in nanotechnology for cancer treatment. *Urol. Oncol.* **2008**, *26* (1), 74–85.
- (11) Yoo, J. W.; Doshi, N.; Mitragotri, S. Adaptive micro and nanoparticles: temporal control over carrier properties to facilitate drug delivery. *Adv. Drug Delivery Rev.* **2011**, *63* (14–15), 1247–1256.
- (12) Elsbahy, M.; Wooley, K. L. Design of polymeric nanoparticles for biomedical delivery applications. *Chem. Soc. Rev.* **2012**, *41* (7), 2545–2561.
- (13) Nie, S.; Xing, Y.; Kim, G. J.; Simons, J. W. Nanotechnology applications in cancer. *Annu. Rev. Biomed. Eng.* **2007**, *9*, 257–288.

- (14) Koo, H.; Huh, M. S.; Sun, I. C.; Yuk, S. H.; Choi, K.; Kim, K.; Kwon, I. C. In vivo targeted delivery of nanoparticles for theranosis. *Acc. Chem. Res.* **2011**, *44* (10), 1018–1028.
- (15) Petros, R. A.; DeSimone, J. M. Strategies in the design of nanoparticles for therapeutic applications. *Nat. Rev. Drug Discovery* **2010**, *9* (8), 615–627.
- (16) Byrne, J. D.; Betancourt, T.; Brannon-Peppas, L. Active targeting schemes for nanoparticle systems in cancer therapeutics. *Adv. Drug Delivery Rev.* **2008**, *60* (15), 1615–1626.
- (17) Fang, J.; Nakamura, H.; Maeda, H. The EPR effect: Unique features of tumor blood vessels for drug delivery, factors involved, and limitations and augmentation of the effect. *Adv. Drug Delivery Rev.* **2011**, *63* (3), 136–151.
- (18) Prabhakar, U.; Maeda, H.; Jain, R. K.; Sevik-Muraca, E. M.; Zamboni, W.; Farokhzad, O. C.; Barry, S. T.; Gabizon, A.; Grodzinski, P.; Blakey, D. C. Challenges and key considerations of the enhanced permeability and retention effect for nanomedicine drug delivery in oncology. *Cancer Res.* **2013**, *73* (8), 2412–2417.
- (19) Feng, L.; Mumper, R. J. A critical review of lipid-based nanoparticles for taxane delivery. *Cancer Lett.* **2013**, *334* (2), 157–175.
- (20) Betancourt, T.; Byrne, J. D.; Sunaryo, N.; Crowder, S. W.; Kadapakkam, M.; Patel, S.; Casciato, S.; Brannon-Peppas, L. PEGylation strategies for active targeting of PLA/PLGA nanoparticles. *J. Biomed. Mater. Res. A* **2009**, *91* (1), 263–276.
- (21) Jokerst, J. V.; Lobovkina, T.; Zare, R. N.; Gambhir, S. S. Nanoparticle PEGylation for imaging and therapy. *Nanomedicine (London)* **2011**, *6* (4), 715–728.
- (22) Muller, R. H.; Mader, K.; Gohla, S. Solid lipid nanoparticles (SLN) for controlled drug delivery - a review of the state of the art. *Eur. J. Pharm. Biopharm.* **2000**, *50* (1), 161–177.
- (23) Venkateswarlu, V.; Manjunath, K. Preparation, characterization and in vitro release kinetics of clozapine solid lipid nanoparticles. *J. Controlled Release* **2004**, *95* (3), 627–638.
- (24) Yang, S. C.; Lu, L. F.; Cai, Y.; Zhu, J. B.; Liang, B. W.; Yang, C. Z. Body distribution in mice of intravenously injected camptothecin solid lipid nanoparticles and targeting effect on brain. *J. Controlled Release* **1999**, *59* (3), 299–307.
- (25) Schwarz, C.; Mehnert, W.; Lucks, J. S.; M+ller, R. H. Solid lipid nanoparticles (SLN) for controlled drug delivery. I. Production, characterization and sterilization. *J. Controlled Release* **1994**, *30* (1), 83–96.
- (26) Mehnert, W.; Mader, K. Solid lipid nanoparticles: production, characterization and applications. *Adv. Drug Delivery Rev.* **2001**, *47* (2–3), 165–196.
- (27) Xu, Z.; Chen, L.; Gu, W.; Gao, Y.; Lin, L.; Zhang, Z.; Xi, Y.; Li, Y. The performance of docetaxel-loaded solid lipid nanoparticles targeted to hepatocellular carcinoma. *Biomaterials* **2009**, *30* (2), 226–232.
- (28) Gao, Y.; Yang, R.; Zhang, Z.; Chen, L.; Sun, Z.; Li, Y. Solid lipid nanoparticles reduce systemic toxicity of docetaxel: performance and mechanism in animal. *Nanotoxicology* **2011**, *5* (4), 636–649.
- (29) Xu, W.; Lim, S. J.; Lee, M. K. Cellular uptake and antitumor activity of paclitaxel incorporated into trilaurin-based solid lipid nanoparticles in ovarian cancer. *J. Microencapsulation* **2013**, *30* (8), 755–761.
- (30) Lee, M. K.; Lim, S. J.; Kim, C. K. Preparation, characterization and in vitro cytotoxicity of paclitaxel-loaded sterically stabilized solid lipid nanoparticles. *Biomaterials* **2007**, *28* (12), 2137–2146.
- (31) Heurtault, B.; Saulnier, P.; Pech, B.; Proust, J. E.; Benoit, J. P. A novel phase inversion-based process for the preparation of lipid nanocarriers. *Pharm. Res.* **2002**, *19* (6), 875–880.
- (32) Peltier, S.; Oger, J. M.; Lagarce, F.; Couet, W.; Benoit, J. P. Enhanced oral paclitaxel bioavailability after administration of paclitaxel-loaded lipid nanocapsules. *Pharm. Res.* **2006**, *23* (6), 1243–1250.
- (33) Lacoueille, F.; Hindre, F.; Moal, F.; Roux, J.; Passirani, C.; Couturier, O.; Cales, P.; Le Jeune, J. J.; Lamprecht, A.; Benoit, J. P. In vivo evaluation of lipid nanocapsules as a promising colloidal carrier for paclitaxel. *Int. J. Pharm.* **2007**, *344* (1–2), 143–149.
- (34) Li, R.; Eun, J. S.; Lee, M. K. Pharmacokinetics and biodistribution of paclitaxel loaded in pegylated solid lipid nanoparticles after intravenous administration. *Arch. Pharm. Res.* **2011**, *34* (2), 331–337.
- (35) Videira, M. A.; Arranja, A. G.; Gouveia, L. F. Experimental design towards an optimal lipid nanosystem: a new opportunity for paclitaxel-based therapeutics. *Eur. J. Pharm. Sci.* **2013**, *49* (2), 302–310.
- (36) Huynh, L.; Grant, J.; Leroux, J. C.; Delmas, P.; Allen, C. Predicting the solubility of the anti-cancer agent docetaxel in small molecule excipients using computational methods. *Pharm. Res.* **2008**, *25* (1), 147–157.
- (37) Chan, J. M.; Zhang, L.; Yuet, K. P.; Liao, G.; Rhee, J. W.; Langer, R.; Farokhzad, O. C. PLGA-lecithin-PEG core-shell nanoparticles for controlled drug delivery. *Biomaterials* **2009**, *30* (8), 1627–1634.
- (38) Zhu, S.; Lansakara, P.; Li, X.; Cui, Z. Lysosomal Delivery of a Lipophilic Gemcitabine Prodrug Using Novel Acid-Sensitive Micelles Improved Its Antitumor Activity. *Bioconjugate Chem.* **2012**, *23* (5), 966–980.
- (39) Yanasarn, N.; Sloat, B. R.; Cui, Z. Nanoparticles engineered from lecithin-in-water emulsions as a potential delivery system for docetaxel. *Int. J. Pharm.* **2009**, *379* (1), 174–180.
- (40) Tao, W.; Zeng, X.; Liu, T.; Wang, Z.; Xiong, Q.; Ouyang, C.; Huang, L.; Mei, L. Docetaxel-loaded nanoparticles based on star-shaped mannitol-core PLGA-TPGS diblock copolymer for breast cancer therapy. *Acta Biomater.* **2013**, *9* (11), 8910–8920.
- (41) Sloat, B. R.; Sandoval, M. A.; Li, D.; Chung, W. G.; Lansakara, P.; Proteau, P. J.; Kiguchi, K.; DiGiovanni, J.; Cui, Z. In vitro and in vivo anti-tumor activities of a gemcitabine derivative carried by nanoparticles. *Int. J. Pharm.* **2011**, *409* (1–2), 278–288.
- (42) Kim, D. W.; Kim, S. Y.; Kim, H. K.; Kim, S. W.; Shin, S. W.; Kim, J. S.; Park, K.; Lee, M. Y.; Heo, D. S. Multicenter phase II trial of Genexol-PM, a novel Cremophor-free, polymeric micelle formulation of paclitaxel, with cisplatin in patients with advanced non-small-cell lung cancer. *Ann. Oncol.* **2007**, *18* (12), 2009–2014.
- (43) Lee, K. S.; Chung, H. C.; Im, S. A.; Park, Y. H.; Kim, C. S.; Kim, S. B.; Rha, S. Y.; Lee, M. Y.; Ro, J. Multicenter phase II trial of Genexol-PM, a Cremophor-free, polymeric micelle formulation of paclitaxel, in patients with metastatic breast cancer. *Breast Cancer Res. Treat.* **2008**, *108* (2), 241–250.
- (44) Shi, J.; Xiao, Z.; Kamaly, N.; Farokhzad, O. C. Self-assembled targeted nanoparticles: evolution of technologies and bench to bedside translation. *Acc. Chem. Res.* **2011**, *44* (10), 1123–1134.
- (45) Mikhail, A. S.; Allen, C. Poly(ethylene glycol)-b-poly(epsilon-caprolactone) micelles containing chemically conjugated and physically entrapped docetaxel: synthesis, characterization, and the influence of the drug on micelle morphology. *Biomacromolecules* **2010**, *11* (5), 1273–1280.
- (46) Farokhzad, O. C.; Langer, R. Impact of nanotechnology on drug delivery. *ACS Nano* **2009**, *3* (1), 16–20.
- (47) Torchilin, V. Tumor delivery of macromolecular drugs based on the EPR effect. *Adv. Drug Delivery Rev.* **2011**, *63* (3), 131–135.
- (48) Iyer, A. K.; Khaled, G.; Fang, J.; Maeda, H. Exploiting the enhanced permeability and retention effect for tumor targeting. *Drug Discovery Today* **2006**, *11* (17–18), 812–818.
- (49) Maeda, H.; Bharate, G. Y.; Daruwalla, J. Polymeric drugs for efficient tumor-targeted drug delivery based on EPR-effect. *Eur. J. Pharm. Biopharm.* **2009**, *71* (3), 409–419.
- (50) Kraus, L. A.; Samuel, S. K.; Schmid, S. M.; Dykes, D. J.; Waud, W. R.; Bissery, M. C. The mechanism of action of docetaxel (Taxotere) in xenograft models is not limited to bcl-2 phosphorylation. *Invest. New Drugs* **2003**, *21* (3), 259–268.
- (51) Fang, J.; Sawa, T.; Maeda, H. Factors and mechanism of “EPR: effect and the enhanced antitumor effects of macromolecular drugs including SMANCS. *Adv. Exp. Med. Biol.* **2003**, *519*, 29–49.
- (52) Wang, L.; Li, M.; Zhang, N. Folate-targeted docetaxel-lipid-based-nanosuspensions for active-targeted cancer therapy. *Int. J. Nanomed.* **2012**, *7*, 3281–3294.

(53) Liu, D.; Liu, F.; Liu, Z.; Wang, L.; Zhang, N. Tumor specific delivery and therapy by double-targeted nanostructured lipid carriers with anti-VEGFR-2 antibody. *Mol. Pharmaceutics* **2011**, *8* (6), 2291–2301.

(54) Liu, D.; Liu, Z.; Wang, L.; Zhang, C.; Zhang, N. Nanostructured lipid carriers as novel carrier for parenteral delivery of docetaxel. *Colloids Surf, B* **2011**, *85* (2), 262–269.

(55) Mi, Y.; Zhao, J.; Feng, S. S. Targeted co-delivery of docetaxel, cisplatin and herceptin by vitamin E TPGS-cisplatin prodrug nanoparticles for multimodality treatment of cancer. *J. Controlled Release* **2013**, *169* (3), 185–192.

(56) Westesen, K.; Bunjes, H. Do nanoparticles prepared from lipids solid at room temperature always possess a solid lipid matrix? *Int. J. Pharm.* **1995**, *115* (1), 129–131.

(57) Yerlikaya, F.; Ozgen, A.; Vural, I.; Guven, O.; Karaagaoglu, E.; Khan, M. A.; Capan, Y. Development and Evaluation of Paclitaxel Nanoparticles Using a Quality-by-Design Approach. *J. Pharm. Sci.* **2013**, *102* (10), 3748–3761.

(58) Bunjes, H.; Westesen, K.; Koch, M. H. J. Crystallization tendency and polymorphic transitions in triglyceride nanoparticles. *Int. J. Pharm.* **1996**, *129* (1–2), 159–173.

(59) Wasutrasawat, P.; Al-Obaidi, H.; Gaisford, S.; Lawrence, M. J.; Warisnoicharoen, W. Drug solubilisation in lipid nanoparticles containing high melting point triglycerides. *Eur. J. Pharm. Biopharm.* **2013**, *85* (3), 365–371.

(60) Mosallaei, N.; Jaafari, M. R.; Hanafi-Bojd, M. Y.; Golmohammadzadeh, S.; Malaek-Nikouei, B. Docetaxel-loaded solid lipid nanoparticles: preparation, characterization, in vitro, and in vivo evaluations. *J. Pharm. Sci.* **2013**, *102* (6), 1994–2004.

(61) Li, X.; Wang, D.; Zhang, J.; Pan, W. Preparation and pharmacokinetics of docetaxel based on nanostructured lipid carriers. *J. Pharm. Pharmacol.* **2009**, *61* (11), 1485–1492.

(62) Wang, S.; Koo, S. I. Plasma clearance and hepatic utilization of stearic, myristic and linoleic acids introduced via chylomicrons in rats. *Lipids* **1993**, *28* (8), 697–703.